Available online at www.sciencedirect.com
ScienceDirect
Journal of the European Ceramic Society 29 (2009) 77–83
www.elsevier.com/locate/jeurceramsoc

Microstructural development of $SrAl_{12}O_{19}$ in alumina–strontia composites

K. Vishista *, F.D. Gnanam

Department of Physics, Anna University, Chennai 600025, India

Received 10 June 2007; received in revised form 4 May 2008; accepted 17 May 2008
Available online 21 July 2008

Abstract

Boehmite sol was prepared by hot water hydrolysis of aluminium *iso*-propoxide using nitric acid as catalyst. Strontium nitrate was added to the boehmite sol to yield 0-20 vol.% strontia. The boehmite with additives was dried at 120 °C. The powder samples were calcined at 1600 °C for 3 h and the formation of strontium hexa-aluminate is discussed using phase diagram, transmission electron microscope and energy dispersive spectra. The powder samples calcined at 500 °C were milled for 6 h, compacted into cylindrical pellets using uni-axial press at 180 MPa and sintered at 1600 °C for 6 h. A microstructural model was proposed for the formation of strontium hexa-aluminate. The sintered pellets were ground and phases determined using XRD. The formation of hexa-aluminate (plate-like) grains was confirmed using optical microscope and scanning electron micronscope.

Keywords: Al_2O_3; Composites; Strontia; Hexa-aluminate; Sol-gel

1. Introduction

The microstructural properties of ceramics can be controlled by incorporating a second phase as dispersed particulates and/or platelets.[1] Composites containing whiskers, fibres and platelets as second phase are difficult to sinter to high density without expensive hot pressing or hot isostatic pressing so that the applications are limited. Alumina ceramic composites formed through the sol–gel route with particles or whiskers as reinforcement may exhibit fine-grained microstructure, which leads to high mechanical properties, combined with chemical stability.[2–4]

The "in situ" second phase formation during sintering leads to novel microstructure and hence has attracted much attention in recent years.

Tsukuma and Takahata[5] added a small amount of La_2O_3 to 2Y-TZP/Al_2O_3 to form $LaAl_{11}O_{18}$ platelets. The resultant composite had higher fracture toughness and higher strength at high temperatures as compared to the base 2Y-TZP/Al_2O_3. Cutler et al.[6] used SrO as the additive in Ce-TZP/Al_2O_3 to form "in situ" platelets of $SrAl_{12}O_{19}$ obtaining an attractive combination of high levels of strength, toughness and hardness. Chen and Chen[7] reported benefits and limitations of "in situ" formed aluminate platelets. Park et al.[8] observed plate-like abnormal grain growth in WC-Co/Al_2O_3 composites. Kang et al.[9] observed the abnormal grain growth in $BaTiO_3$/Al_2O_3 composites, Kim et al.[10] reported abnormal grain growth behaviour in Al_2O_3/SiC composites; Ree et al.[11] reported similar observations in Al_2O_3/Si_3N_4 composites; Choi et al.[12] reported angular grains in TaC–TiC–Ni composites. Mullite containing angular grains by the addition of certain additives has also been reported.[13] Vishista et al.[24] reported the formation of calcium hexa-aluminate grains by the addition of calcia to alumina. The morphology of sintered alumina varies significantly with type of impurities such as magnesia, calcia, silica, soda and baria.[14]

The addition of strontium oxide to alumina in the ratio of 1:6 yields strontium hexa-aluminate, a compound of formula $SrAl_{12}O_{19}$ (SA_6). A characteristic feature of SA_6 is its strongly anisotropic growth, which results in elongated grains and platelets. Virkar et al.[15] have shown that the addition of SrO to alumina/zirconia (Al_2O_3/ZrO_2) composites leads to materials with fracture toughness of 14–15 MPa $m^{1/2}$, strength of 500–700 MPa and hardness of 14–15 GPa. Stefano Maschio and Pezzotti[16] reported similar results when SrO is

* Corresponding author.
E-mail address: vishista@yahoo.com (K. Vishista).

0955-2219/$ – see front matter © 2008 Elsevier Ltd. All rights reserved.
doi:10.1016/j.jeurceramsoc.2008.05.041

added to a system constituted by alumina–chromia/zirconia (Al_2O_3–Cr_2O_3/ZrO_2).

The plate-like morphology of strontium hexa-aluminate increases the mechanical properties of alumina ceramics.[22] Hence this paper deals with the study of the microstructural development and the mechanism of "in situ" formation of strontium hexa-aluminate in alumina–strontia composites.

2. Experimental procedure

Boehmite sol was prepared by hot water hydrolysis of aluminium *iso*-propoxide. Hydrolysis was carried out using double distilled water by stirring for 1 h at 80 °C. Nitric acid was added as peptizing agent. Peptization was carried out with vigorous stirring for 1 h at 80 °C. Then strontium nitrate was added to yield 0–20 vol.% of strontia. Both hydrolysis and peptization were performed under reflux conditions reducing the loss of material. Boehmite sol with additives was precipitated in ammonia, aged overnight, vacuum filtered, oven dried at 120 °C for 2 days and calcined at 500 °C for 3 h. The calcined powder was ground in a planetary mill at 230 rpm for 6 h. Particle size analysis was performed using Laser particle size analyzer Shimadzu SALD 1100 model. The powder samples were calcined at 1600 °C/3 h and TEM studies were performed using JEOL 3000 FX high resolution Transmission Electron Microscope (HRTEM). The powder was compacted into cylindrical pellets using uni-axial press at 180 MPa and sintered at temperatures ranging from 1400 to 1600 °C for 6 h. X-ray powder diffraction spectra were observed for the sintered samples (ground) on Philips analytical diffractometer PW 3710 model using Cu Kα radiation. The samples were scanned from 20° to 80° (2θ) (high angle XRD). The pellets were mirror polished, thermally etched, coated with gold using POLORON 500 sputter coating unit and then analyzed using Leica LEO Stereoscan 440 scanning electron microscope (SEM) under secondary electron (SE) mode.

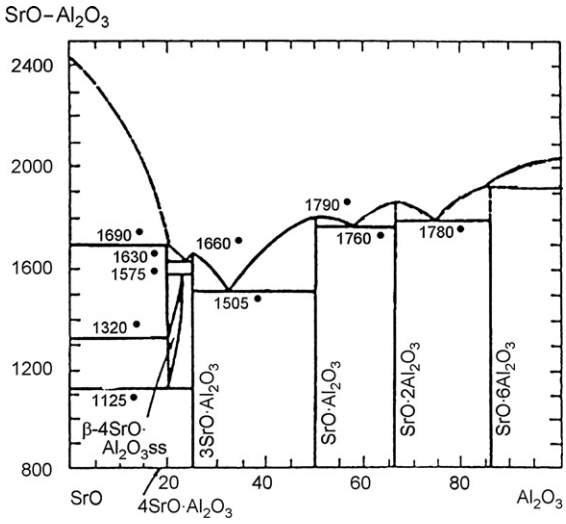

Fig. 1. Phase diagram of SrO–Al_2O_3 system.

3. Results and discussion

3.1. SrO–Al_2O_3 phase diagram

The SrO–Al_2O_3 system shown in Fig. 1 has five binary phases: $3SrO{\cdot}Al_2O_3$, $SrO{\cdot}Al_2O_3$, $SrO{\cdot}2Al_2O_3$, $4SrO{\cdot}Al_2O_3$ and $SrO{\cdot}6Al_2O_3$. Liquidus temperatures drop rapidly upon addition of Al_2O_3 to SrO. Thus, $SrO{\cdot}6Al_2O_3$ melts incongruently to Al_2O_3 at 1920 °C. The minimum melting compositions are the eutectics between

(i) $SrO{\cdot}2Al_2O_3$ and $SrO{\cdot}6Al_2O_3$ located at 1780 °C.
(ii) $SrO{\cdot}Al_2O_3$ and $SrO{\cdot}2Al_2O_3$ located at 1760 °C.
(iii) $3SrO{\cdot}Al_2O_3$ and $SrO{\cdot}Al_2O_3$ located at 1505 °C.
(iv) α-$4SrO{\cdot}Al_2O_3$ and $3SrO{\cdot}Al_2O_3$ located at 1630 °C.

It is noteworthy that phase relations in this area can be conveniently studied using the classical quenching techniques

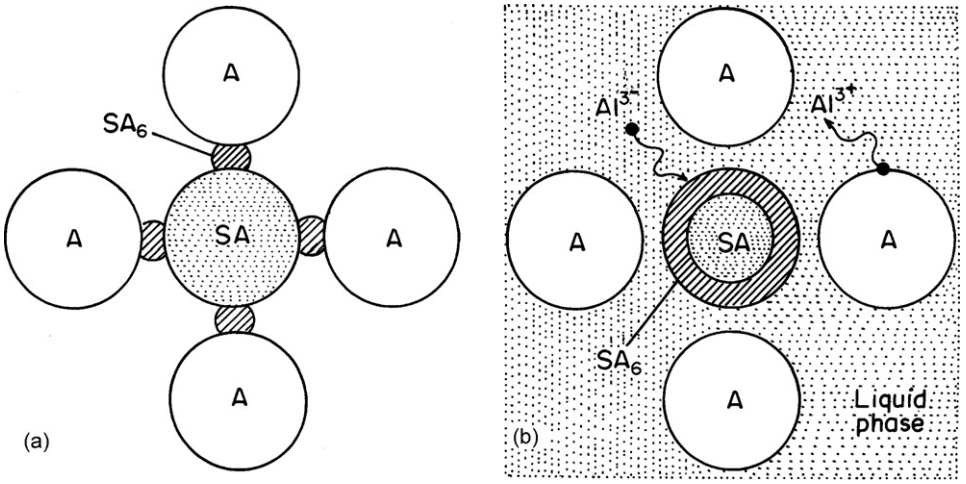

Fig. 2. Microstructural model for Al_2O_3–SrO composite.

because the strontium aluminate liquids quench readily to yield glasses. The non-silicate glasses are formed because the aluminate liquids have random-network structures built up of (AlO_4) tetrahedra, analogous to the random-network structures based on (SiO_4) tetrahedral that are encountered in silicate liquids and glasses.

3.2. Microstructural model

During the early stages of sintering, monostrontium aluminate is formed by solid-state reaction between strontia and alumina in the powder compact. Hexa-aluminate must be formed by further reaction between SA and alumina. Which can occur by two distinct mechanisms as shown in Fig. 2. One possibility is that the SA_6 nucleates at the interfaces between alumina and SA particles and the reaction proceeds by solid-state diffusion through the reactant phase. However, if the surfaces of the SA_6 and the alumina grains were already wet by a liquid phase, the transformation to SA_6 would, by necessity, take place via solution-precipitation reaction. The reaction by solid-state diffusion results in the formation of equiaxed SA_6 grains, where solution-precipitation favours the development of plate-like grains. It is proposed that localized melting takes place as a result of low temperature eutectic reaction in the $SrO–Al_2O_3$ system and it is this eutectic liquid which plays the dominant role in affecting the SA_6 reaction mechanism (similar model is proposed by An et al. for the alumina–calcia system).[17] The difference in the final microstructure lies in the extent to which solid-state reaction has occurred between SA and SA_6 prior to wetting by the liquid phase. This will depend on a variety of factors including particle size, packing density and uniform dispersion (mixing) of the alumina–strontia powders. A slight difference in the above factors could have an appreciable effect on the subsequent wetting behaviour and microstructure development. SA_6 may be formed by

(i) the reaction between SrO (S) and Al_2O_3 (A) obtained in the reaction mix by the low temperature dissolution of strontia and gamma alumina;
(ii) the reaction between S and A;
(iii) the reaction between SA_2 and A;
(iv) the reaction among SA, SA_2 and A.

The equations representing the probable reactions for the formation of strontium hexa-aluminate are represented as follows:

$$S + 6A \rightarrow SA_6$$

$$SA + 5A \rightarrow SA_6$$

$$SA_2 + 4A \rightarrow SA_6$$

$$SA + SA_2 + 9A \rightarrow 2SA_6$$

$$2SA + SA_2 + 14A \rightarrow 3SA_6$$

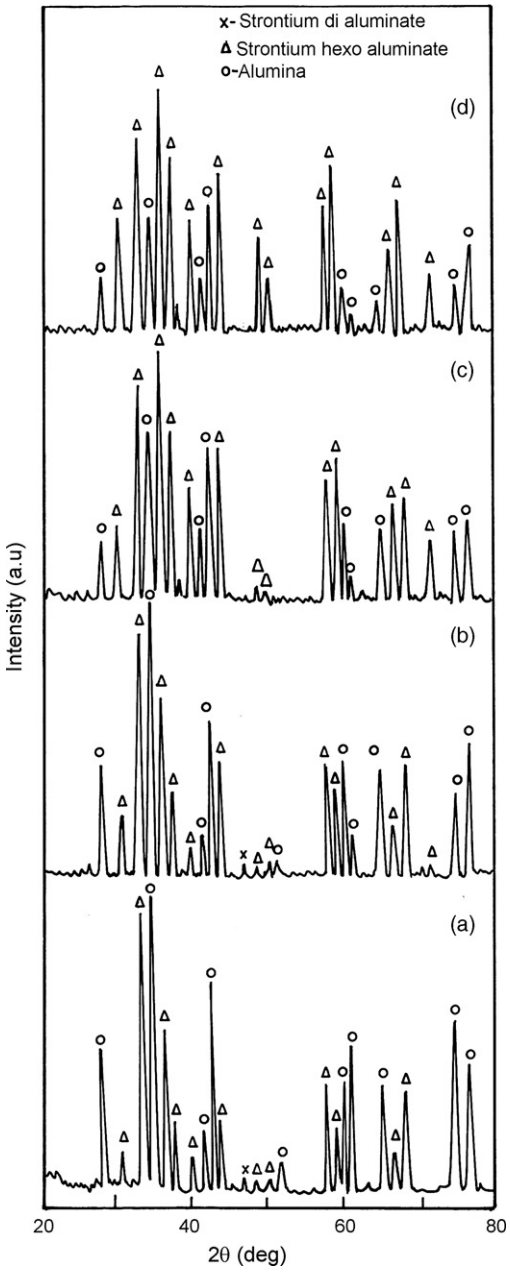

Fig. 3. XRD pattern of alumina with (a) 5 vol.% SrO, (b) 10 vol.% SrO, (c) 15 vol.% SrO and (d) 20 vol.% SrO.

SA and SA_2 are both reaction intermediates and are minimised with the formation of SA_6. Similar reaction intermediates were proposed for formation of calcium aluminates.[18,19]

3.3. XRD: phases identification

The samples with different concentrations of strontia sintered at 1600 °C/6 h were ground and the phases were identified by XRD analysis. Fig. 3 shows the XRD patterns for different concentrations of alumina/strontia composites. The presence of different strontium aluminates was confirmed by comparing the values of the observed peaks with their standard values as per

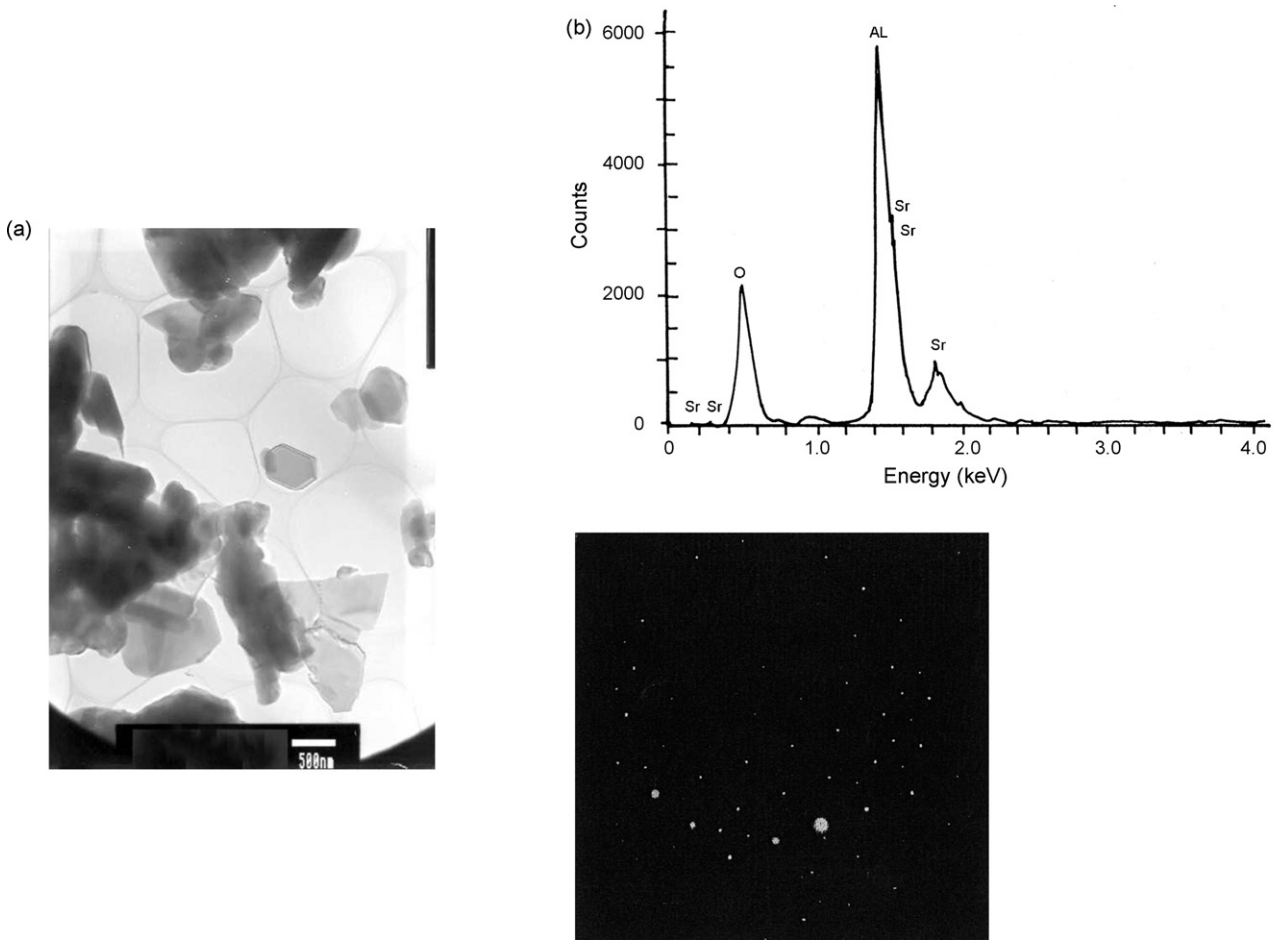

Fig. 4. TEM and EDS of Al_2O_3–10 vol.% SrO composite powders.

JCPDS. It is found that with the increase in the SrO content, the strontium hexa-aluminate phase becomes prominent. With the phase diagram of the SrO–Al_2O_3 system (Fig. 1) the different phases SA_6, Al_2O_3 and SA_2 were noted. The presence of these phases were observed using XRD when the strontia content was varied from 10 to 20 vol.%. The formation of strontium aluminates has also been reported using the impregnation method.[20]

3.4. Particle size analysis

A starting powder of high chemical purity, with small median particle size, narrow particle size distribution, controlled pore size and pore size distribution are essential for obtaining controlled microstructure and improved mechanical properties. The particle size analysis of the powders containing 0, 5, 10, 15 and 20 vol.% strontia was performed using laser diffraction particle size analyzer. Narrow particle size distribution was observed. The average particle size was found to increase with the amount of strontia, when the other processing parameters were unaltered. The results of the particle size analysis for various concentrations of strontia calcined at 1600 °C/3 h are given in Table 1.

3.5. TEM and EDS studies

The size and location of the strontia particles in the composite powder were analysed using high resolution transmission electron microscopy (HRTEM) and energy dispersive spectra (EDS). Fig. 4(a and b) shows the results of the TEM and EDS observations of alumina–10 vol.% strontia composite powders calcined at 1600 °C/3 h. The calcination temperature is chosen such that both the alumina and strontium hexa-aluminate grains are formed. It can be seen that the alumina crystallites are hexagonal in shape and are in the size range of 100-500 nm. The strontium hexa-aluminate crystallites are platelets in shape and are in the size range of 3-3.5 μm. The EDS spectrum is taken

Table 1
Particle size analysis for various concentrations of strontia

Concentration of strontia (vol.%)	Average particle size (μm)
0	2.68
5	2.8
10	2.97
15	3.03
20	3.3

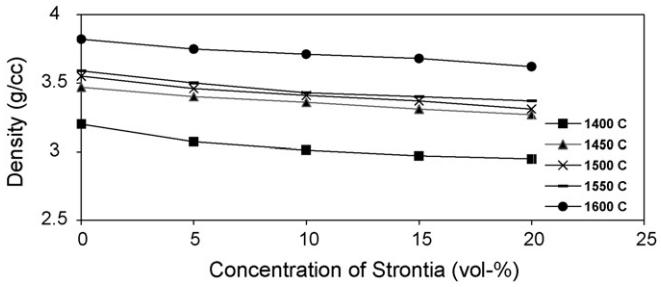

Fig. 5. Dependence of density on concentration of strontia.

on the composite powder focussed on the alumina particles with strontia particles in its surroundings.

3.6. Density studies

The density studies were performed on the sintered pellets by Archemedes method (using dry weight, soaked weight and suspended weight). Fig. 5 shows the density as a function of concentrations of strontia for different sintering temperatures. The sintering temperature was varied from 1400° to 1600 °C. The density is found to increase with the increase in the sintering temperature. However, there is a slight decrease in density with increase in strontia content. The slight decrease in the sintered density is due to the formation of strontium hexa-aluminate plate-like grains. Since the pores are trapped within or between the large grains, further densification is hindered and hence the decrease in density.[22] Similar densification is reported for calcia by Goswami et al.[14] and Vishista and Gnanam.[23]

When the additive concentration is within the solubility limit, the homogeneous mixing accelerates the densification by diffusion phenomena. Considering the relationship between the Al^{3+} and Sr^{2+}, in the alumina lattice position is the most possible solid-state mechanism. The majority of the pores remained located at the grain boundaries. Pore boundary separations occur, but not always within the large abnormal grains. The strontia added to alumina shows a uniform microstructure of highly homogeneous distribution. The additive shows very fine equiaxed and elongated grains. Large elongated grains are the main features of the microstructure.

Polished cross sections viewed under SEM shows an increasing tendency to form plate-shaped grains with increasing SrO additions.

3.7. Microstructure

The samples were polished and thermally etched for optical and SEM studies. Fig. 6(a–d) shows the optical micrographs of alumina −with 5-20 vol.% strontia composites. The plate-like grains are clearly visible. The samples viewed under SEM show plate-shaped grains with the addition of SrO as shown in Fig. 7(a–e). The micrographs show that the composites have increasing tendency of forming plate-like grains with increasing strontia additions. The aspect ratio of the grains increases with the concentration of SrO. This suggests that strontium hexa-aluminate (hexagonal $SrO{\cdot}6Al_2O_3$) is formed in situ during sintering, as expected from the phase equilibria of $SrO–Al_2O_3$ system. The microstructure shows that the strontium hexa-aluminate grains are platelets. The $SrAl_{12}O_{19}$ platelets, are approximately 2–3 μm in width and 5–10 μm in length.

The anisotropic grain growth was enhanced as seen in the microstructure with the increase in strontia content. The fine equiaxed microstructure observed for pure alumina was completely replaced by a new set of large faceted grains. The

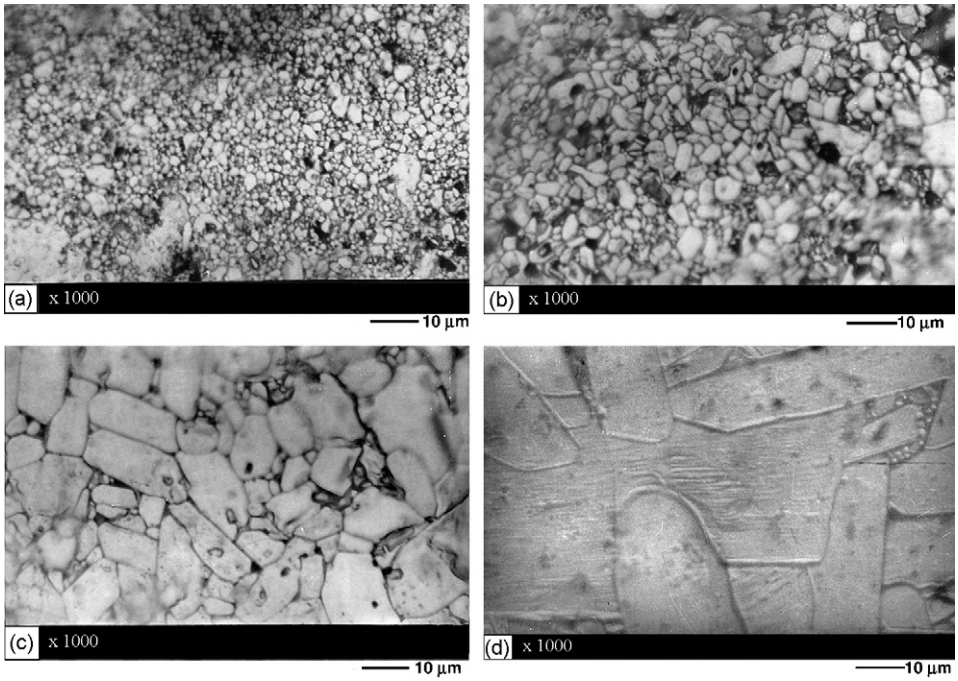

Fig. 6. Optical micrographs of alumina with (a) 5 vol.% SrO, (b) 10 vol.% SrO, (c) 15 vol.% SrO and (d) 20 vol.% SrO composites.

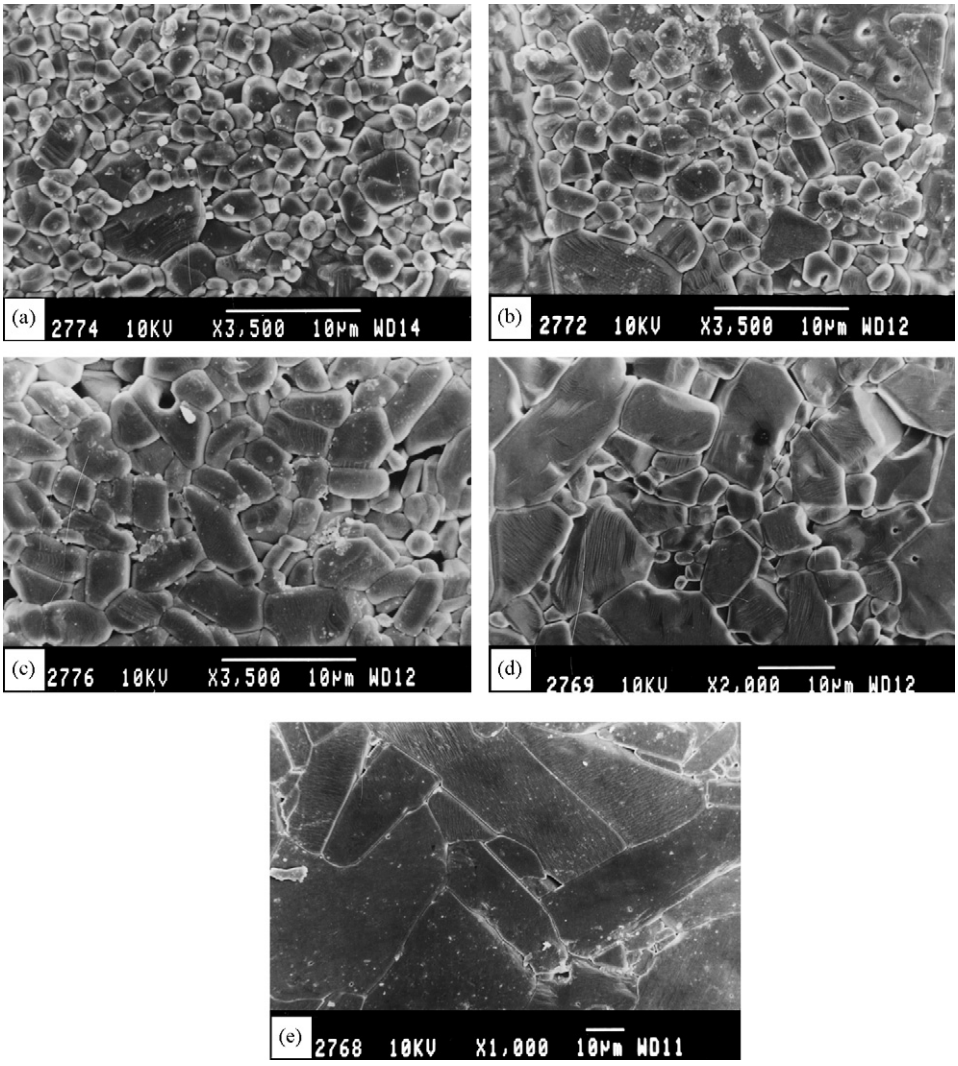

Fig. 7. SEM pictures of alumina with (a) 0 vol.% SrO, (b) 5 vol.% SrO, (c) 10 vol.% SrO, (d) 15 vol.% SrO and (e) 20 vol% SrO.

resultant microstructure was fine and uniform as many grains grow simultaneously. Because of the increase in strontia content, the number of abnormally growing plate-like grains becomes large. One method to increase the toughness of ceramic materials has been the inclusion of secondary phases that interact with a propagating crack and remain unfractured at the crack tip while exerting a crack closure stress as result of bridging the crack wake. Such materials exhibit a rising *R*-curve behaviour and are related to the magnitude of bridging stresses in the crack wake and have been experimentally verified by in situ microscopic observations. While a sharp increase in fracture toughness has been obtained through the incorporation of continuous fibres, the inclusion of platelet or needle like grains that develop in situ during sintering/densification has the advantage of reduced processing time and cost while still providing reasonable increase in toughness (Sbaizero).[21] Crack propagation takes place through alumina grains; alumina platelets, along alumina grain boundaries and along phase interfaces. At higher volume fraction of aluminates, crack bridging by aluminate ligaments is to be observed frequently. The toughness of the composites increases with increase in grain size up to a critical grain size.

4. Conclusions

(a) Alumina–strontium hexa-aluminate composites were synthesised by the sol–gel technique.
(b) The powders were characterised using TEM and EDS the presence of alumina and strontium hexa-aluminate were confirmed.
(c) X-ray diffraction analysis confirmed the presence of the strontium hexa-aluminate, strontium di-aluminate, and alumina phases.
(d) The microstructural model for the development of strontium hexa-aluminate grains was proposed.
(e) The microstructural analysis shows that the equiaxed alumina grains were replaced by elongated plate-like strontium hexa-aluminate grains with the increasing strontia concentration.

References

1. Sekino, Tohru, Yu, Ji-Hun, Choa, Yong-Ho, Lee, Jai-Sung and Niihara, Koichii, Reduction and sintering of alumina/tungsten nano composites. *J. Ceram. Jpn.*, 2000, **108**(6), 45–47.
2. Yang, Quanzu and Troczynski, Tom, Dispersion of alumina and Silicon carbide powders in alumina sol. *J. Am. Ceram. Soc.*, 1999, **82**(7), 1928–1930.
3. An, Lian and Chan, Helen M., R-Curve behavior of in situ toughened $Al_2O_3/CaAl_{12}O_{19}$ ceramic composites. *J. Am. Ceram. Soc.*, 1999, **79**(12), 1342–1349.
4. Tzing, W. H. and Tuan, W. H., Exaggerated grain growth of Fe doped alumina. *J. Mater. Sci. Lett.*, 1990, **18**, 1115–1117.
5. Tsukuma, K. and Takahata, T., Mechanical properties and microstructure of TZP/TZP–Al_2O_3 composites. *Mater. Res.*, 1987, **78**, 123–135.
6. Cutler, R. A., Mayhew, R. J., Prettyman, K. M. and Virkar, A. V., High toughness Ce-TZP/Al_2O_3 ceramics with improved hardness and strength. *J. Am. Ceram. Soc.*, 1991, **74**(1), 1709–1786.
7. Chen, Pei-Lin and Chen, I-Wei, In situ alumina/aluminate platelet composites. *J. Am. Ceram. Soc.*, 1992, **75**(9), 2610–2612.
8. Park, Y. J., Hwang, N. M. and Yoon, D. Y., AGG of faceted grains in Co liquid matrix. *Metal. Trans.*, 1996, **27A**, 2809–2819.
9. Kang, M. K., Yoo, Y. S., Kim, D. Y. and Hwang, N. M., Growth of $BaTiO_3$ grains by the twin-plate re-entrant edge mechanism. *J. Am Ceram. Soc.*, 2000, **83**(2), 385–390.
10. Kim, Y. W., Kim, J. Y., Ree, S. H. and Kim, D. Y., Effect of initial particle size on microstructure of liquidphase sintered silicon carbide. *J. Eur. Ceram. Sci.*, 2000, **20**(7), 945–949.
11. Ree, S. H., Lee, J. D. and Kim, D. Y., Effect of heating rate on the exaggerated grain growth behaviour of Si_3N_4. *Mater. Lett.*, 1997, **32**, 115–120.
12. Choi, K., Choi, J. W., Kim, D. Y. and Hwang, N. M., Effect of coalescence on the grain coarsening during liquid phase sintering of TaC–TiC–Ni cermets. *Acta Mater.*, 2000, **48**(12), 3125–3129.
13. Song, S. H. and Messing, G. L., AGG in diphasic Gel-derived Titania doped Mullite. *J. Am. Ceram. Soc.*, 1998, **81**(5), 1269–1277.
14. Goswami, Amiya P., Roy, Sukumar, Mithra, Manoj K. and Gopes, C. D., Impurity dependent morphology and grain growth in liquid phase sintered alumina. *J. Am. Ceram. Soc.*, 2001, **84**(7), 1620–1626.
15. Virkar, A. V., Cutler, R. A., Mayhew, R. J. and Prettyman, K. M., High Toughness Ce-TZP/Al_2O_3 ceramics with improved hardness and strength. *J. Am. Ceram. Soc.*, 1991, **74**(1), 179–186.
16. Maschio, Stefano and Pezzotti, Giuseppe, Microstructure development and Mechanical properties of alumina-hex-aluminate composites as-sintered and after aging in aqueous physiological solution. *J. Ceram. Soc. Jpn.*, 1999, **107**(3), 270–274.
17. An, L., Chan, H. M. and Soni, K. K., Control of Calcium hexaluminate grain morphology in in-situ toughened ceramic composites. *J. Mater. Sci.*, 1996, **31**, 3223–3229.
18. Singh, Vipin Kant, Sintering of calcium aluminate mixes. *Brit. Ceram. Trans.*, 1999, **98**(4), 1213–1216.
19. Singh, Vipin Kant and Sharma, Krishna Kumar, Low temperature synthesis of calcium hexa-aluminate. *J. Am. Ceram. Soc.*, 2002, **84**(9), 769–772.
20. Okada, Kiyoshi, Hattori, Akiyoshi, Taniguchi, Taketoshi, Nukui, Akihiko and Das, Rathindra Nath, Effect of divalent cation additives on the γ–α alumina phase transition. *J. Am. Ceram. Soc.*, 2000, **83**(4), 928–932.
21. Sbaizero, O., Maschio, S., Pezzotti, G. and Davies, I. J., Microprobe Flourescence spectroscopy evaluation of stress fields developed along a propagating crack in an $Al_2O_3/CaO{\cdot}6Al_2O_3$ ceramic composites. *J. Mater. Res.*, 2001, **16**(10), 2798–2802.
22. Vishista, K. and Gnanam, F. D., Effect of Strontia on the densification and mechanical properties of sol-gel alumina. *Ceramics International*, 2006, **32**, 917–922.
23. Vishista, K. and Gnanam, F. D., Effect of calcia on the densification and mechanical properties of sol-gel alumina. *Transactions of the Indian Ceramic society*, 2006, **65**(1), 17–21.
24. Vishista, K., Awaji, H. and Gnanam, F. D., sol–gel synthesis and characterisation of alumina–calcium hexaluminate composites. *J. Am. Ceram. Soc.*, 2005, **88**(5), 1175–1179.